Weather and Climate Extremes 37 (2022) 100471

Contents lists available at ScienceDirect

Weather and Climate Extremes

journal homepage: www.elsevier.com/locate/wace

Heat and cold waves in mainland Spain: Origins, characteristics, and trends

Roberto Serrano-Notivoli [a,*], Marc Lemus-Canovas [b], Samuel Barrao [c], Pablo Sarricolea [d], Oliver Meseguer-Ruiz [e], Ernesto Tejedor [f]

[a] Departamento de Geografía, Universidad Autónoma de Madrid, Madrid, Spain
[b] Andorra Research + Innovation, Sant Julià De Lòria, Andorra
[c] Department of Geography and Regional Planning, University of Zaragoza, Zaragoza, Spain
[d] Department of Geography, University of Chile, Santiago, Chile
[e] Departamento de Ciencias Históricas y Geográficas, Universidad de Tarapacá, Sede Iquique, Chile
[f] Department of Atmospheric and Environmental Sciences, University at Albany, United States

ARTICLE INFO

Keywords:
Heat wave
Cold wave
Climatic variability
Synoptic classification
Spain

ABSTRACT

Heat and cold waves are extreme temperature events with a high potential of causing negative impacts on human health, and natural and socioeconomic systems, depending on their duration and intensity. There is, however, no consensual approach to address their definition, which is critical to set priority action areas to prevent such risks. Mainland Spain experiences heat and cold waves every year with important impacts especially in the most populated areas with mild or transition climates. Here we used a high-resolution (5 × 5 km) gridded daily temperature dataset and employed a combination of threshold exceedances of maximum and minimum temperature in the same day to identify heat and cold wave events over 75 years (1940–2014). We further examined the duration and the seasonal/annual intensities to detect potential spatial and temporal patterns. Additionally, we used the days within the most widespread events to perform a synoptic classification to categorise the atmospheric conditions leading to high-risk situations. Our results show a similar historical duration of heat and cold waves (4–5 days) and a much higher seasonal intensity of cold ones (double than heat waves). We find a tipping point in the early 1980s from which heat waves became more frequent, longer, and more intense than cold waves. Finally, we discern between 9 historical weather types with a dominance of southern advections driving heat waves and cold continental north-northeast air masses causing cold waves. Understanding the patterns and trends of heat and cold waves, as well as the mechanisms of their genesis is key to assist in risk management in mainland Spain, especially in the context of a warming climate scenario.

1. Introduction

Extreme temperatures do not only occur as isolated short events but in continued several-day episodes, leading to compound impacts on human health and environmental and societal systems, such as water resources, crop yields, or electricity consumption, amongst others. Heat and cold waves (HWs and CWs hereinafter) are considered hazards that have different effects depending on their duration, magnitude, and frequency, but also on the exposure of people and goods, and the vulnerability of the territory based on its climatic resilience. For this reason, it is important to understanding how HWs and CWs can impact on different climatic environments and their potential prediction based on a robust knowledge of their most frequent origins and behaviours (Fischer and Schär, 2010; Hu et al., 2019).

In this regard, the definition of when HWs and CWs begin and end cannot be constrained to the univariate climatic perspective of threshold-exceeding consecutive days, but it should also consider the potential effects on these systems. Due to the complex chain of events triggered by an extreme temperature event, this consideration relies on the interrelated characteristics of HWs and CWs (e.g., duration and intensity), stressing out the necessity of addressing them concurrently (AghaKouchak et al., 2020). To this end, a multivariate approach using maximum and minimum temperature is key to consider the whole picture of extreme temperature occurrences. For example, many HWs studies, focused on maximum temperature, limit the understanding of the phenomena to the central hours of the day, which completely ignore the effects of heat at night-time, that have a more intense impact on human well-being (Patz et al., 2005; Tan et al., 2010; Olcina-Cantos

* Corresponding author.
E-mail address: roberto.serrano@uam.es (R. Serrano-Notivoli).

https://doi.org/10.1016/j.wace.2022.100471
Received 30 November 2021; Received in revised form 20 February 2022; Accepted 2 June 2022
Available online 4 June 2022

et al., 2019). Thus, addressing both maximum and minimum temperatures allow for a better representation of the impacts on morbidity and mortality and helps in health alerts responses and prevention (Montero et al., 2010). In this regard, the use of frequency distributions (FD) instead of fixed absolute temperature thresholds for HWs and CWs definition is recommended since they better adapt to future climatic variability and climatic change (Radinović and Ćurić, 2012).

In addition, the usual approach to study HWs and CWs implies the analysis over individual meteorological observatories based on long-term data series. Although it is a practical approach with reliable results, it is subject to the spatial distribution of the observatories, which is not spatially balanced or representative of all types of climates or temperature regimes. In fact, most of the longest data series belong to urban observatories, that are more likely to induce non-natural variations in data because of changes in land cover over time. Gridded datasets offer a continuous representation of climatic variables that, depending on the spatial and temporal resolution as well as the number of observations used to create them, provide reliable and representative climatic information of any spatial domain (Serrano-Notivoli and Tejedor, 2021). The use of gridded temperatures for HWs/CWs analyses has been barely explored except for global or large-region purposes (e.g., Perkins et al., 2012; Lavaysse et al., 2019; Liu et al., 2021) or at finer scales (e.g., Spinioni et al., 2015) and yet, grids can provide a real advantage if they were built on a strong basis due to: 1) the information of all the observations (not only the longest data series) is considered; 2) the value at each grid-box includes the local temperature from the nearby station and also a regional variation from nearby observatories that are used to calculate the temperature estimate; 3) the urban effect is partly removed since data is not exclusive from cities but it is modelled from a collection of adjacent observations. While these premises could reduce the values of the absolute extremes in comparison with the observations, it is, in fact, insignificant because a reliable grid using all the available information offers a similar frequency distribution in the estimates than in the observations.

Gridded datasets are especially useful in regions with strong temporal and spatial variations of temperature, such as mainland Spain (González-Hidalgo et al., 2021). From arid environments in the south, including maximum absolute temperatures exceeding 40 °C, to minimum absolutes temperatures below −10 °C in the north (Serrano-Notivoli et al., 2019), the duration of HWs and CWs can last for more than one week in both cases (Pereira et al., 2017). Some previous works have addressed the spatial distribution of these phenomena (e.g. Prieto et al., 2004; Abaurrea et al., 2018; Acero et al., 2017), however, the above-mentioned issues are still not resolved. Mainland Spain requires a thorough and precise definition of extreme temperature drivers and characteristics to provide tailored territorial plans that consider the climatic variability according to socioeconomic activities.

In this work, we study the spatial distribution of HWs and CWs in mainland Spain in terms of frequency, duration, and intensity. The threshold exceedance of extreme maximum and minimum temperatures is considered at the same time, based on a high-resolution daily gridded dataset (5 × 5 km). Additionally, we classified the days within these events in a synoptic climatology to explain their potential atmospheric drivers. Finally, we calculated the temporal trends in frequency, duration, and intensity for both type of events.

2. Material and methods

2.1. Data

Daily maximum and minimum temperature data for the period 1940–2014 were retrieved for mainland Spain from the STEAD dataset (Serrano-Notivoli et al., 2019), which provides quality-controlled and serially-complete data series across the whole Spanish territory in a 5 km horizontal resolution gridded dataset. While this dataset comprises temperature estimates and the HW/CW definition is based on extreme temperature occurrences, the absence of observations might be considered as a bias due to a smoothness in high-values prediction. However, the accuracy and reliability of STEAD is proven and solid since it was built from 5520 observatories through a thorough analysis of local temperature variations, leading to high correlations (Pearson >0.95) and low discrepancies (MAE <0.75) between observations and estimates in the cross-validation process. Details on grid creation and validation can be consulted in Serrano-Notivoli et al. (2019).

2.2. Heat and cold waves calculation

We computed the duration and intensity of HWs and CWs for the 20,242 data series corresponding with all the grid points following the method proposed by Lavaysse et al. (2018) in three stages: 1) Definition of hot (HDs) and cold days (CDs); 2) Detection of HWs and CWs from consecutive HDs and CDs, respectively; and 3) Calculation of seasonal (I_S) and annual (I_A) intensities for all of them.

2.2.1. HD/CD definition

The thresholds from which a day was considered a HD or a CD were independently determined for every day of the study period. In a first stage, daily maximum (T_X) and minimum (T_N) temperatures were transformed into quantiles based on the calendar percentiles of each variable for all years, using a 7-day moving window. Despite the high number of years (75), we included in this calculation the 3 prior and subsequent days to the target day with the aim of strengthening the thresholds based on percentiles. This method let us determine a HD/CD based on a 7-day moving window, using a total of 525 values for each day of the study period. We did not consider the target year in the calculation. Thus, a day was defined as HD (CD) when maximum and minimum temperatures were higher (lower) than the 90th (10th) percentile of that day.

2.2.2. HW/CW detection

When at least 3 consecutive HDs (CDs) were found, a HW (CW) was flagged. This threshold, which is widely accepted in climate studies (Robinson, 2001; Smith et al., 2013; Pascal et al., 2013) and noted by the WMO, is also the official minimum temporal range adopted by the Spanish meteorological agency (AEMET) to consider the occurrence of a HW (CW). While we did not impose a maximum temporal threshold for waves duration, a gap of one day in HDs/CDs occurrence was accepted, meaning that two or more waves separated by one day were merged in a single one. However, we did not consider these linking days in the duration or intensity calculations.

Following Lavaysse et al. (2018), the year was divided in two periods and HWs were only considered from April to September, the hottest half of year, while CWs where considered from October to March, just to find the cold events with higher impacts. Based on the statistical classification, HWs (CWs) can occur out of these periods, but their frequency and incidence are much lower and, thus, we did not take them into consideration.

2.2.3. HW/CW intensities

Once the waves were detected for all grid points, two different measures of intensity were calculated:

The seasonal intensity (I_S) was defined as the accumulated temperature anomaly during a wave with respect to the climatological daily thresholds:

$$I_S = \sum_{i=1}^{N} \beta \frac{\left(T_{X_{i,w}} - Q_{T_X}\right) + \left(T_{N_{i,w}} - Q_{T_N}\right)}{2}$$

$$\begin{cases} \beta = 1 \, for \, HW \\ \beta = -1 \, for \, CW \end{cases}$$

where N is the duration of the wave in days (except linking days), $T_{X_{i,w}}$

and $T_{N_{i,w}}$ are the maximum and minimum temperatures recorded at days i within the wave for grid point w, and Q_{T_X} and Q_{T_N} are the temperatures for the quantile 0.9 (0.1) of the days of the HW (CW). This approach is useful to account for anomalies contextualized in the period of occurrence of the wave, having a great importance in key economic activities in Spain, such as crop development, ripening (e.g., HWs are critical in viticulture from July to September) or tourism (e.g., both HWs and CWs have great impacts on beach and skiing tourism, respectively).

The annual intensity (I_A) was based on the same approach, quantifying the temperature exceedance, but in this case using a constant threshold:

$$I_A = \sum_{i=1}^{N} \beta \left[\frac{\left(T_{X_{i,w}} - T_{X_{med\left(Q_{T_X}\right)}} \right)}{2\sigma_{T_X}} + \frac{\left(T_{N_{i,w}} - T_{N_{med\left(Q_{T_N}\right)}} \right)}{2\sigma_{T_N}} \right]$$

$$\begin{cases} \beta = 1 \; for \; HW \\ \beta = -1 \; for \; CW \end{cases}$$

where $T_{X_{med(Q_{T_X})}}$ and $T_{N_{med(Q_{T_N})}}$ are the temperature (constant) of the median of all calendar daily quantiles of 0.9 (0.1) for HWs (CWs), and the σ_{T_X} and σ_{T_N} are the standard deviation of maximum and minimum temperature data series, respectively. Unlike the seasonal approach, this method considers the intensity of the wave in the context of the complete year, which emphasizes the most intense absolute temperatures. It also helps to evaluate the impacts of those systems and processes with a broader sensitiveness to temperature extremes, or at least those with longer responses, such as tree growth and, of course, the effects on human thermal comfort and health. The seasonal cycle variance consideration helps to soften the intensity of waves in locations with very high seasonal cycle like mountain climates or those with high effects of continentality.

2.2.4. HW/CW trends

With the aim of looking for temporal patterns in the evolution of the frequency, duration, and intensity of the combined occurrence of HWs and CWs, we calculated the rate of change of the difference between both types of events for each variable. We used the linear trend value, indicating the corresponding significance. To extend this analysis, the trends for each variable and type of event are shown in supplementary material (see Figs. S2 and S3).

2.3. Synoptic climatologies

To extract the most typical atmospheric situations of HWs and CWs occurrence, we selected the days in which more than 50% of the study area was affected by a HW/CW to apply the classification. This selection resulted in 165 days for HWs and 228 days for CWs.

In this study, HW and CW days were separately classified by means of a Principal Component Analysis (PCA) approach, a widely used methodology to estimate the most representative synoptic patterns of extreme events (Philipp et al., 2016; Insua-Costa et al., 2021; Lemus-Canovas et al., 2021). We applied the PCA to a temporal mode (T-mode) matrix of 500 hPa geopotential height, mean sea level pressure, and 850 hPa temperature, obtained from ERA5 reanalysis data (Hersbach et al., 2020). Thus, in the T-mode matrix, the variables (columns) were the days within the identified HW or CW events, and the observations (rows) were the grid points from the ERA5 used spatial domain (30°-50°N, 15°W-23°E). We worked with mean daily values: the three variables were obtained every 6 h, and then they were daily averaged to obtain a single value for each day. After applying the PCA to the previously standardized original data matrix, we obtained the new obtained variables (linear combinations of the original variables). We used the Scree Test (Cattell, 1966) to determine the number of components to retain based on the amount of explained variance by each PC. These retained PCs were subsequently rotated by means of a varimax rotation to obtain the maximum variance explained for each PC (Richman, 1986). From the rotated PCs, we obtained the loadings, indicating the degree of correlation of every day with each PC. In this sense, the assignment of each day to each PC (WT) was based on the maximum correlation value (e.g., day 1 was assigned to the PC with the highest (absolute) correlation).

The R package synoptReg (Lemus-Canovas et al., 2019) was used to develop such a classification. After applying this method, each day within a HW or CW was associated with a single weather type.

3. Results

3.1. Heat and cold waves occurrence variability

The spatial distribution of the number of events (Fig. 1) showed a general occurrence of at least one event per year in the whole territory for both HWs and CWs. However, HWs revealed a higher average with more than 2 events per year except for coastal areas, while CW occurrences ranged between 1 and 2 events per year except the highest values at northeast with frequencies over 2 events per year.

HWs (Fig. 1a) showed a clear dominance in the southern half, mainly occupying areas of high elevation, while depressions and coastal areas obtained the lowest values (below 1.5 events per year. For instance, less than 1 event per year occurred in the northern coast under Atlantic influence and in the central Mediterranean coast. The CWs (Fig. 1b), with a general low frequency, rarely showed areas with less than 1 annual event. The higher occurrences were found in northeast IP, over mountain ranges, coinciding also with high occurrences of HWs.

3.2. Duration and intensity of HW and CW

Regarding the duration of the events, HWs and CWs showed a similar spatial pattern (Fig. 2a, d): a general duration of 4–5 days with longer events (>5 days) in south eastern IP. Only in some coastal areas of HWs, duration was lower than 4 days per event.

The intensity, expressed as the excess of Celsius degrees in a seasonal and in an annual basis, showed large differences, but all of them had in common a virtual diagonal separation from northwest to southeast, displaying different behaviours of intensity. At seasonal scale (Fig. 2b, e) average values were 7.3 °C and 9.8 °C for HWs and CWs, respectively. HWs showed a gradient from lower to higher intensities from Mediterranean coast to northwest IP. The seasonal intensity of the CW (Fig. 2e) was particularly noteworthy, with very high values in most of peninsular Spain and exceeding 10 °C in almost the entire eastern half. Despite having lower values in occurrence (Fig. 1), CW reached higher intensity values than the HW, meaning that, at seasonal scale, CWs are less frequent but more intense.

Annual intensity evidenced a complementary spatial pattern between HWs and CWs, driven by the diagonal separation. Although both types of events showed a similar average, near to 5 °C, HWs showed higher values at southwest and very low values (<4 °C) in northeast half of the IP, especially in central Mediterranean and northern Cantabric coasts. CWs reached the higher intensities in the northeast side, except for low values at high elevations areas.

When comparing the duration and intensities of HWs and CWs in 3 cities with very different temperature regimes, the dissimilarities in the characteristics of the events become evident. Fig. 3 shows the frequency distributions of the variables for Almeria, a coastal city at the extreme southeast of the IP, with a warm semi-arid climate; Barcelona, a large city at northeast coast with a mild Mediterranean climate; and Santander, a mid-sized city at northern coast with a heavy oceanic influence. Barcelona and Santander (mild temperatures) showed, in average, low durations and intensities, meaning that the most severe HWs, such as the August 2003 event (red arrows in Fig. 3) represented exceptional values compared to the normal characteristics. However, the same event in Almeria was not outstanding in regard of duration and

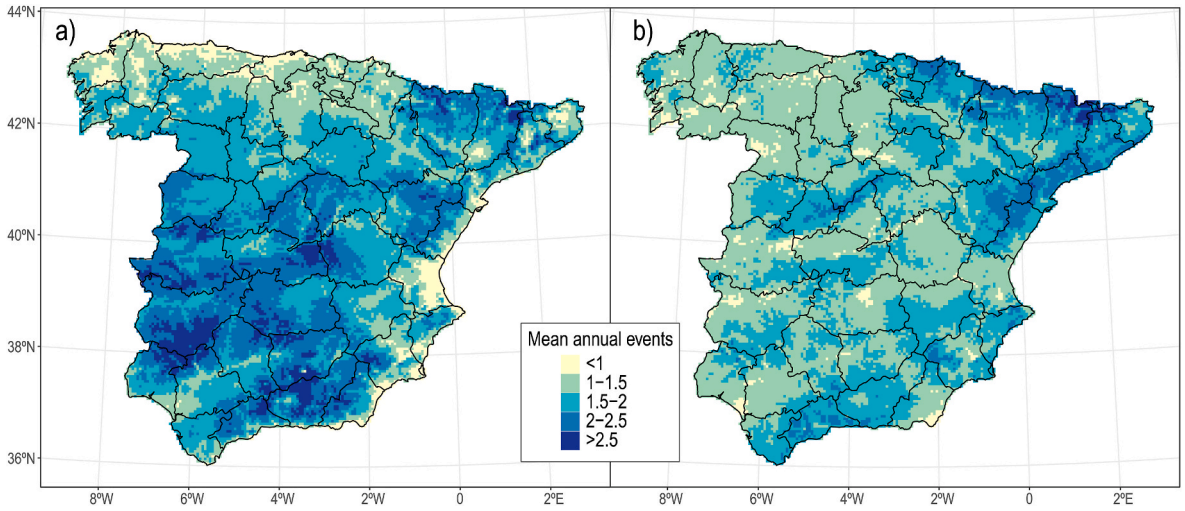

Fig. 1. Mean annual number of HW (left) and CW (right) events.

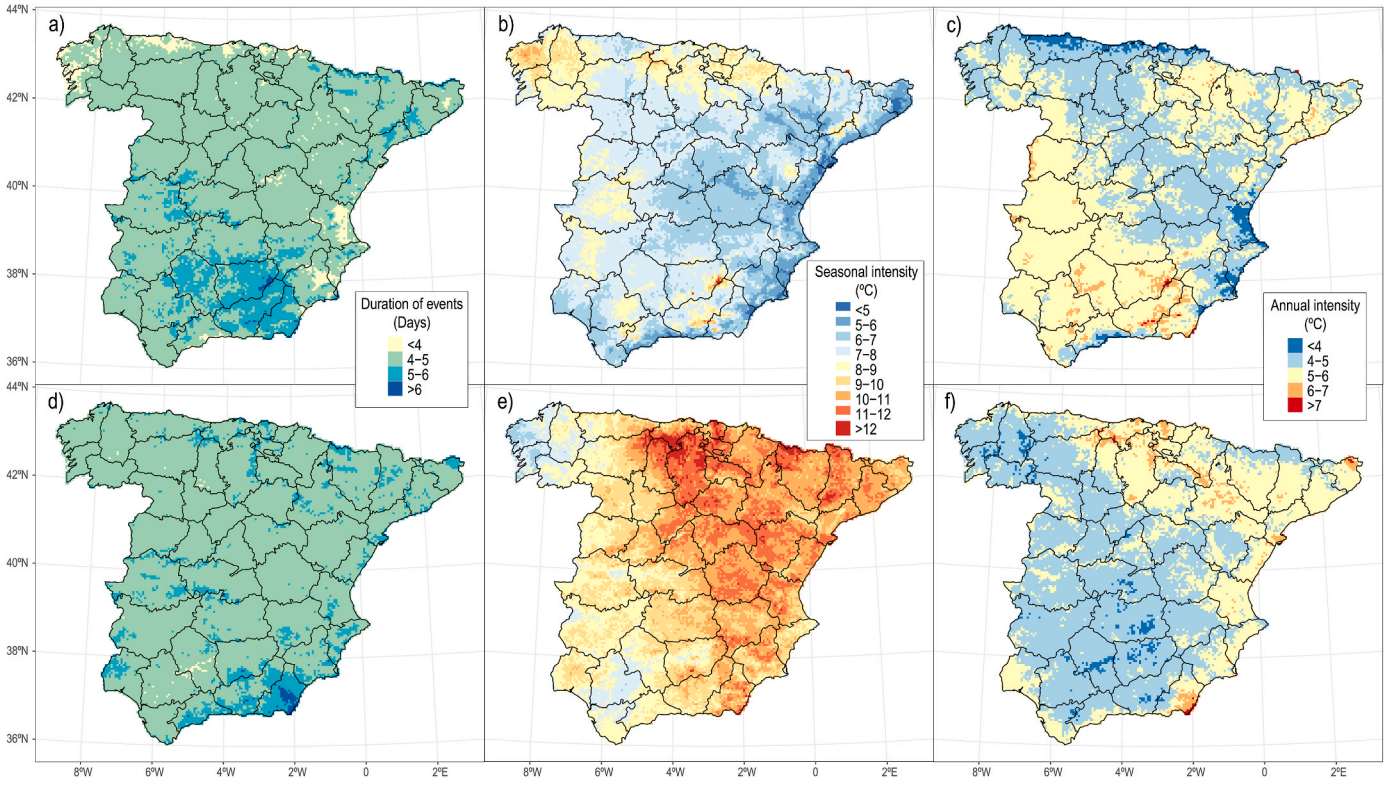

Fig. 2. Duration (a, d), seasonal (b, e) and annual (c, f) intensity of heat (a, b, c) and cold (d, e, f) waves in mainland Spain.

intensity due to the higher frequency of longer and more intense events. Concerning CWs, one of the most extreme events, the cold wave in February 1956, represented in both duration and intensities a much higher magnitude. The duration of the event was from 3 to 7 times higher than usual, and seasonal intensities ranged from 50 °C to 75 °C. The extreme character of these exceptional HW and CW events represents a higher impact on the territory since their wide extension all over the territory (see Fig. S1 at supplementary material).

3.3. Heat and cold waves trends

With respect to the temporal evolution, the difference between the number of annual HWs and CWs (Fig. 4a) showed a positive linear trend of 0.02 events/year for the entire period, meaning that HWs turned into more frequent events than CWs. From 1981 to 2014, the number of HWs was higher than CW all years except two of them (1993 and 2008). Differences in duration (Fig. 4b) followed a similar pattern with a positive trend of 0.03 days/year. However, a reduction of frequency of long duration CWs was noticed (since 1986 only two years exceeded 4-day duration in average, 2001 and 2005). Seasonal and annual intensities also showed positive trends of 0.10 °C/year and 0.05 °C/year, displaying a warming climate in which HWs are becoming more intense than CWs. Still, the progression was not linear. For instance, regarding seasonal intensity (Fig. 4c), from 1940 to 1980, 78% of years reached higher intensities in CWs, while from 1981 to 2014, 56% of years HWs were more intense. In addition, CWs showed a higher frequency of years with

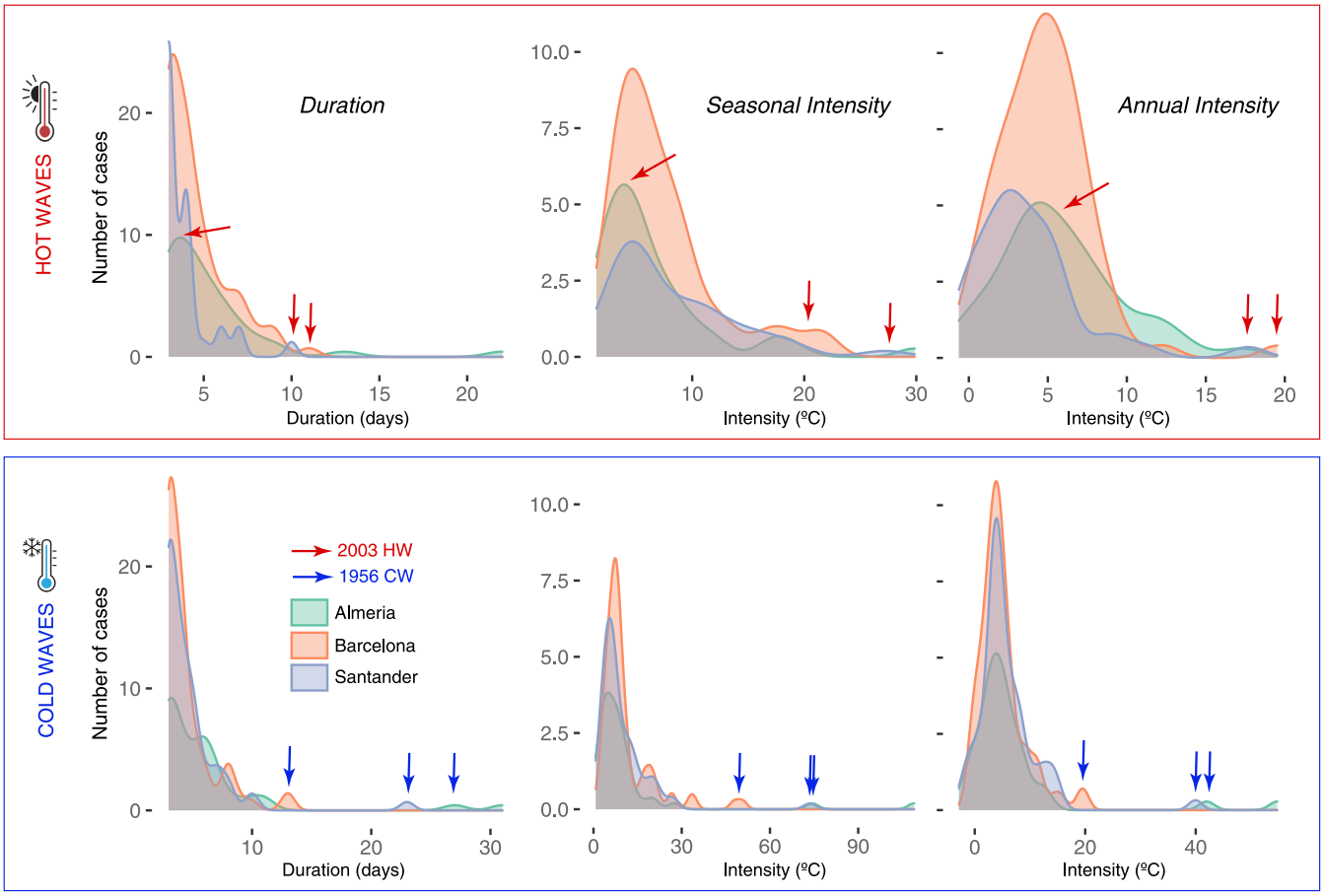

Fig. 3. Average duration, seasonal and annual intensity of hot (upper row) and cold (lower row) waves in 3 cities in Spain. Red and blue arrows indicate the corresponding values of 2003 HW and 1956 CW, respectively. (For interpretation of the references to color in this figure legend, the reader is referred to the Web version of this article.)

very high intensity (>10 °C) (12 until 1980). Annual intensity (Fig. 4d) showed a different temporal pattern, with a clear dominance of higher intensities in HWs from the late 1950s. The interannual variability was higher than the seasonal intensity but, overall, trend values showed a warming direction.

Extreme years (outliers from the average) were more frequent in CWs showing, for example, the 1956 event that highly exceeded the normal values (Fig. S3), but also 1970 and 1983 suffered cold events exceeding 20 °C of seasonal intensity (Fig. 4c). Yet, years such as 1945, 1964 or 1981 were extremely intense in HWs. The year 2003, characterized by several heat waves throughout Europe (e.g., Fink et al., 2004; Burt, 2004), experienced the longest events and the more intense in regard of annual intensities of the entire period.

3.4. Synoptic climatology

Both HWs and CWs are explained by synoptic situations characterized by the advection of air masses from southern and northern latitudes, respectively (Figs. 5 and 6). These situations appear by a diminution of the zonal circulation at 500 hPa, that allow the appearance of anticyclonic ridges and polar troughs.

The classification of all days within HWs and CWs resulted in 9 WT for each type of event.

3.4.1. HW classification

WT1 is relatively frequent over the year (Fig. S4). The months of April, May and June concentrated 82% of these days, mainly in the central month (62%). This WT describes early heat waves, and to a lesser extent, later ones. It is a subtropical ridge situation both at 850 hPa and 500 hPa causing high positive anomalies throughout the Iberian Peninsula. WT2 also reflects mainly premature heat waves (46% in April and 38% in May), but unlike WT1, it has a different structure: the warm intrusion is the result of a subtropical ridge at 500 hPa, but due to an anticyclonic blocking over the British Isles. It mainly affects southwest Iberia. WT3 reflects the same pattern as WT1, but the blocking does not have the same position. In this case, the surface blocking occurs in southern Scandinavia, and this drives a southerly flow favoring a very warm advection up to very northern latitudes. WT4 explains HWs occurring between June and September, centered on the summer months. It shows a very marked subtropical ridge situation, very similar to WT1, but describing another period. WT5 is also a mainly August situation (46%). It shows a subtropical ridge, although there is some blocking between Great Britain, France and Germany. This favors some southerly flow which makes it easier for the very warm air mass to reach further north. WT6 is pretty spread out over time, but most frequent in September, and shows an anticyclonic blocking very clearly at both surface and mid-troposphere. WT7 flash heat in April (4 days, 50%), but also in June (2 days, 25%) and August (2 days, 25%). It causes very intense anomalies over France (Lemus-Cánovas and López-Bustins, 2021). WT8 is more frequent in June (33%), July (25%) and August (21%). It shows a subtropical ridge without a defined surface situation, with a low barometric gradient situation. WT9 is the second least frequent, with 6 days in September and 4 between May and June, just at the beginning and the end of summer months. It is a clear Central

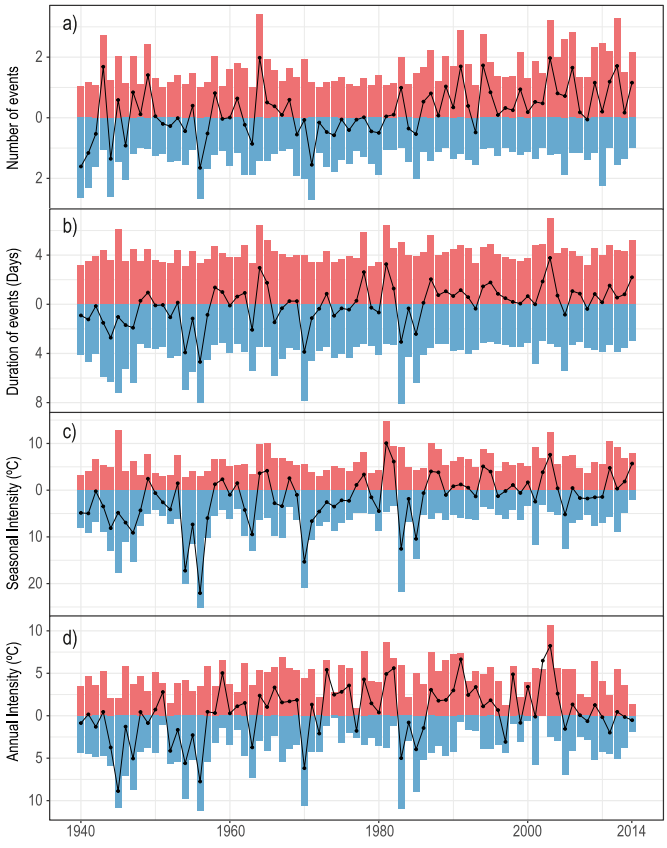

Fig. 4. Average annual number of events (a), duration (b), seasonal intensity (c) and annual intensity (d) of HW (red bars) and CW (blue bars). Black lines show the annual difference in each case. (For interpretation of the references to color in this figure legend, the reader is referred to the Web version of this article.)

European blocking situation.

WT1 was the most frequent (Fig. S5) with more than 40% of cases, especially in northern half of IP. WTs 2, 3, 4 and 8 were very similar with even distributions of frequencies over the territory near to 20%. Below those frequencies, WTs 5, 6, 7, and especially WT9 were the less common, indicating that they are related to very specific situations causing HWs. WT4, which was generalized in 2003 HW, showed a positive significant temporal trend (at the $\alpha = 0.10$ signification level) and WT3 the inverse significant negative trend (Fig. S6).

3.4.2. CW classification

WT1 (Fig. 6) is exclusively a winter pattern, with peak in February (49%) (Fig. S4). This situation shows an extended blocking between Iceland, Great Britain and the Scandinavian Peninsula, opening a very cold continental air corridor with an eastern or northeastern flow. At 500 hPa there is a low pressure in Northeast Iberia. WT2 is fairly distributed, but with a peak in February (33%). It exhibits a blocking situation in the west of the British Isles, which breaks the westerly circulation and facilitates the release of cold air from N-NE. WT3 has a peak in January and February (43% and 30% respectively). The anticyclone over Scandinavia swings southward, favoring a slightly less cold situation in the Iberian Mediterranean, but with a greater contribution of humidity. WT4 is equally distributed, more frequent outside the strictly winter months (October and November). It shows an almost segregated cut-of-low at 500 hPa. WT5 shows a perfect angle of the anticyclonic blocking between Great Britain and Scandinavia, favoring a direct flow from the Siberian area. It is more frequent in January (41%). WT6 is more frequent from the first part of winter through January. In the Mediterranean part it has a very obvious resemblance to WT1, but with no blocking in Northern Europe. The E-NE flow is favored by a momentary rise of the Azores High. It is a less forceful cold wave, since it does not have in favor a long continental path of the air mass. WT7 is more frequent in January (56%), and shows a blocking over Great Britain, causing a short flow, but from the E-NE, with possible humid contribution in the Mediterranean basin. WT8 shows its higher frequency in January (60%), and exhibits a blocking south of Scandinavia. WT9 is an extension of WT1, with a tilting of the blocking over Great Britain to the west and an East-Northeast flow very cold at the surface. Overall, the different variations in atmospheric situations from northern Europe are the responsible for CWs in mainland Spain. Furthermore, the N-NE-E origin is representative of a very probable extreme CW.

WTs 1, 2, 3 and 6 were the most frequent all over the study area (Fig. S7) with more than 30% of occurrences of those atmospheric situations in CWs. WT6 showed the only negative significant (p-value <0.01) trend with a meaningful reduction of occurrences since 1975, while WT7, the less frequent, showed the only positive significant trend (p-value <0.01).

4. Discussion

Heat and cold waves do not have a unique and universal definition. However, its understanding is of paramount importance for risks prediction at different temporal and spatial scales. We used, based on a previous approach (Lavaysse et al., 2018, 2019), the combination of relative exceedances of maximum and minimum temperatures to address the main characteristics of HWs and CWs in mainland Spain. However, this is not the usual method as most of the studies use a univariate way (e.g., Allen and Sheridan, 2016; Bitencourt et al., 2020; Plavcová and Kysely, 2019; Pereira et al., 2017). The main advantage of Lavaysse et al. (2018) approach is that it relativizes the impact of extreme events in relation to the complete range of daily temperatures, constraining the identification of HWs and CWs to the most intense events with higher potential of impact, which is considered based on the intensities at seasonal and annual scale. These two types of intensities accumulate the magnitude of the anomalies throughout the duration of the wave, providing tailored measures of impact to the different natural and human systems. Yet, this is not the only way to address the intensity, for example, Spinioni et al. (2015) considered separately the severity and the intensity, being the latter the ratio between magnitude and duration, which we believe would lead to a reduction of the impact's consideration. In that way, the ratio between a high-magnitude and short-duration wave could result in a similar intensity of a low-magnitude and long-duration wave when, certainly, they do not have the same adverse effects for agriculture or for human organism, amongst others. Seasonal intensity mainly affects the resilience of organisms with shorter life cycles, such as some plants and crops. For instance, crop production can be seriously affected or even suffer a total loss, either by an extreme heat or extreme cold wave that does not need to be extraordinary within the full annual range of historical temperatures. Since these systems are more sensitive to seasonal temperature anomalies, the annual effect is diluted. Instead, the annual intensity has more potential effects on humans and their activities since they are not limited to the range of temperatures of a few months. For example, a hot or cold event which is relatively normal for the season but extraordinary within the full annual temperatures, can have an impact on infrastructures (e.g., power grid, fuel supply, etc.). Nevertheless, seasonal intensities also represent a serious risk for health.

Related to the impacts on different organisms and systems, the type of climate plays a key role on the consideration of an individual event as extraordinary regarding its duration and intensity. Our results showed, in three cities with different temperature regime, how HWs had uneven behavior based on a higher fluctuation of maximum temperatures in comparison to minimum ones. The impact of long and intense HWs was higher in locations with mild climates. However, CWs demonstrated, overall, a higher impact on all territory as shown in Carmona et al.

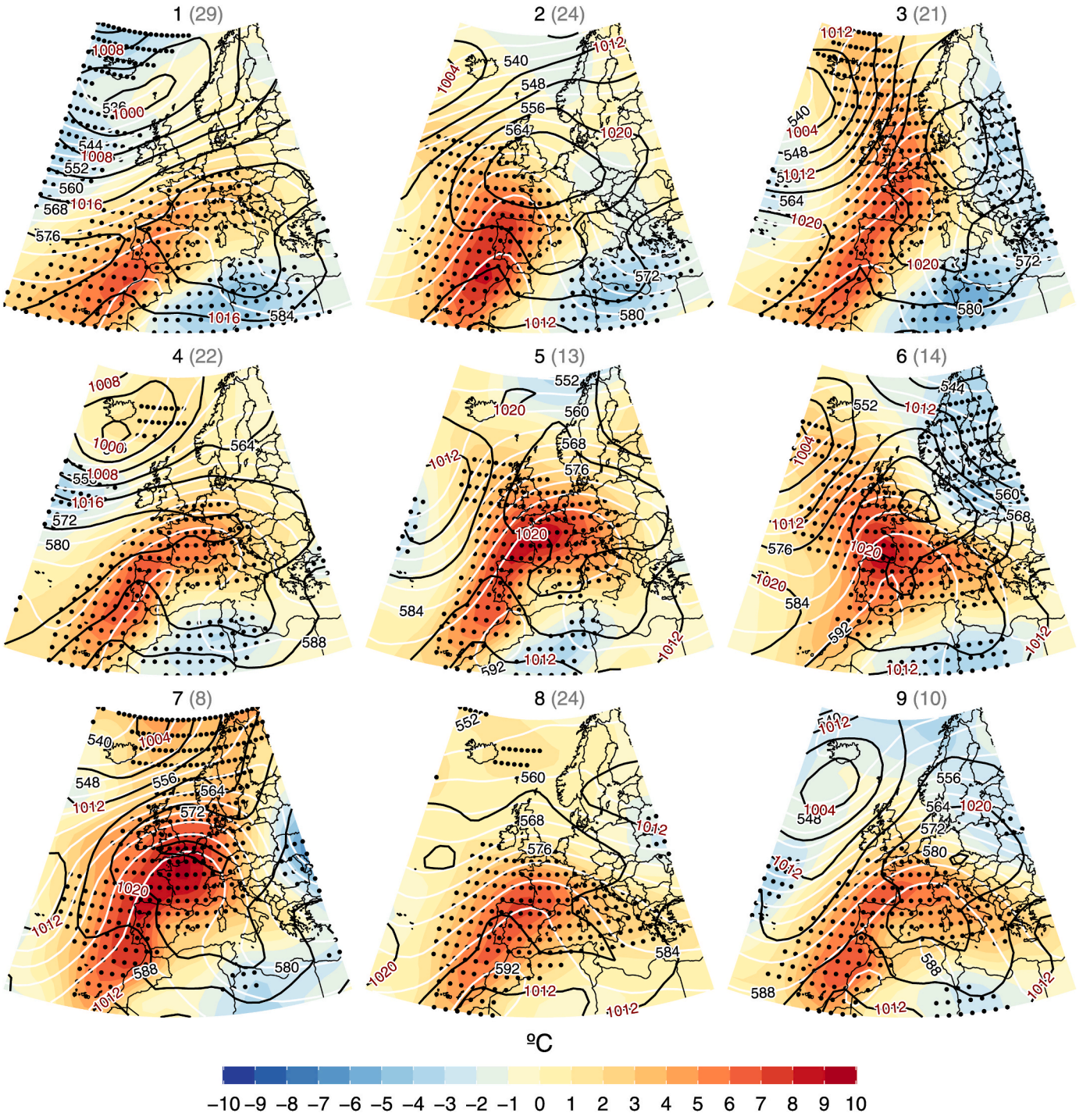

Fig. 5. Synoptic patterns obtained from the classification of days within HW events (gray color, in brackets). Daily anomalies of temperature at 850 hPa (°C, shading), absolute geopotential height at 500 hPa (dm, white contours) with contour interval of 4 dm, and mean sea level pressure (hPa, black contours) with contour interval of 4 hPa. Stippling indicates statistically significant anomalies at the 5% level (two-sided *t*-test). The numeration of each weather type is indicated on the top of each panel. (For interpretation of the references to color in this figure legend, the reader is referred to the Web version of this article.)

(2016) due to the abovementioned lower oscillation of minimum temperatures in mainland Spain (Gutiérrez et al., 2013) and, for this reason, a cold extreme event implies an extraordinary event in almost the entire region. This was observed for the duration and both types of intensities, especially the seasonal, posing a serious risk for the peninsular territory. Yet, trends showed a sustained diminution of CW events over time with a clear tipping point in early 80s, from which HWs became longer and more intense.

These trends agree with recent works addressing past and future evolution of HWs. For instance, Lorenzo et al. (2021) showed a general increase of HWs occurrence in Spain and that high-duration areas did not coincide with high-intensity ones, as shown in our results, and Viceto et al. (2019), using WRF simulations, showed similar spatial patterns in HWs duration and intensity. These works, as most of previous research of HWs/CWs in Spain, used waves detection based on a single variable (maximum or minimum temperature) and on models (GCMs, RCMs) instead of observations. These factors could potentially lead to a higher number of events or intensities. However, Zschenderlein et al.

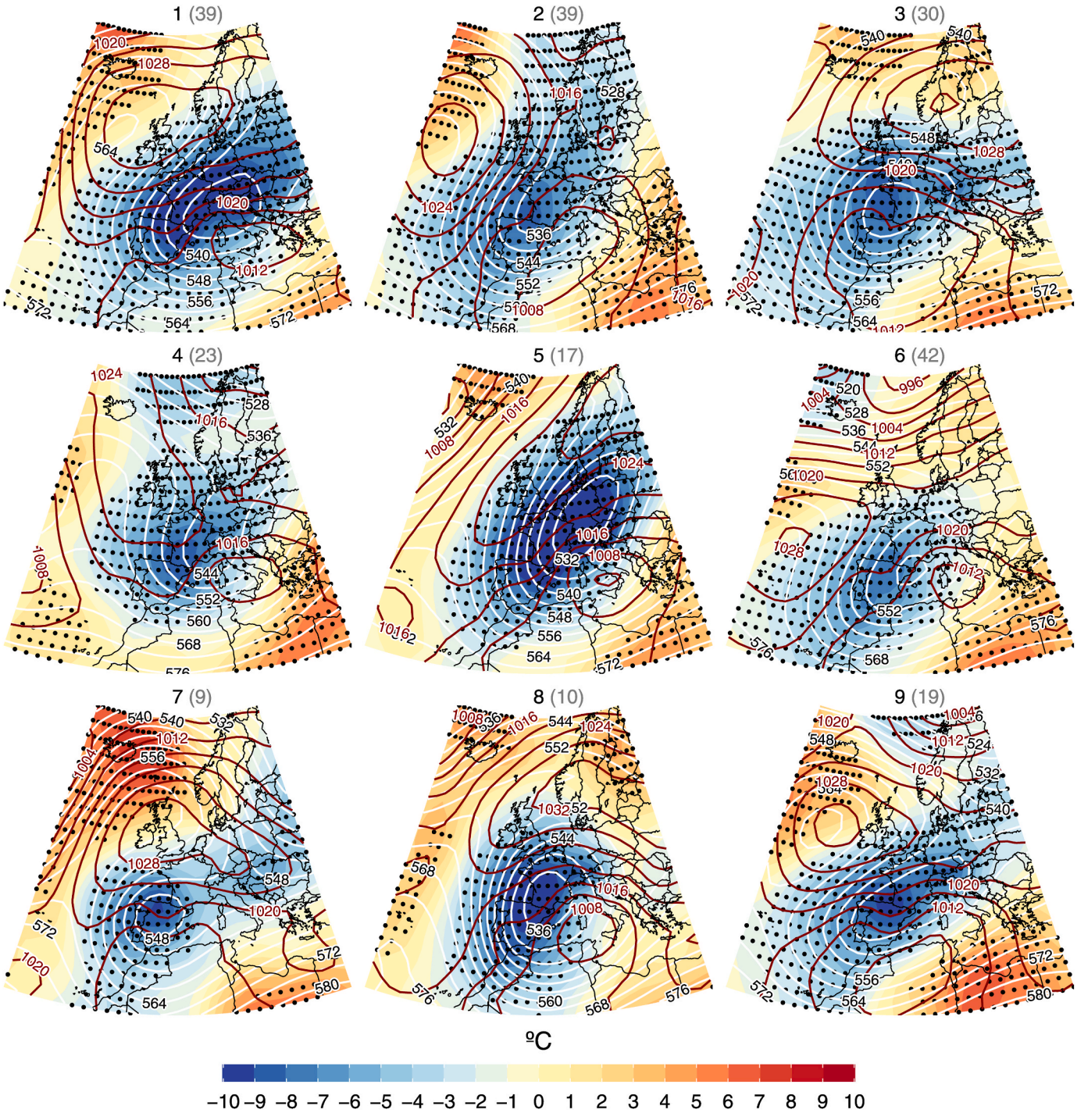

Fig. 6. Same as in Fig. 6, but for CW events.

(2019), using a reanalysis and a HWs detection based only on maximum temperature exceedances, yielded a lower average duration and number of events than our results, probably due to the absence of observations and a low spatial resolution (1°x1°), which have been demonstrated to have a great impact on any resulting calculation (Merino et al., 2021).

While we do not address the causes of the change from 1980s decade towards more HWs prone conditions, a change in the driving atmospheric situations due to global warming is probably behind this alteration. The synoptic classification showed that latitudinal advections of tropical air masses through subtropical ridge situations allowing Saharan warm air were responsible for most of the HW events. These synoptic patterns, shown in all WTs in different ways, is coherent with the configuration detected by Sousa et al. (2019), with different latitudinal extensions. They identified a cyclonic circulation off the coast in the northeastern Atlantic for two extreme HW events in 2018 and 2019 which were out of our study period (1940–2014) and that we did not detect. These conditions could be more frequent in the future and an extension of the study period could reveal more patterns of predictability. For CWs, the different WTs indicated an advection from north to north-east through a corridor, with a relatively low pressure in the Western Mediterranean and, in a few cases, a cut-off-low at 500 hPa over the Iberian Peninsula. These situations also showed a blocking high over Great Britain (Mohammed et al., 2018). The slight differences with other studies are attributed to the different classification methods, but they

just represent non-substantial variations.

This first analysis of the atmospheric drivers of HW/CW events exemplify a static picture already analysed from different perspectives (Sánchez-Benítez et al., 2020) that is, indeed, changing. It would be of key importance to perform an analysis of the persistence of the different WTs to improve the events' characteristics since our results showed changes towards more longer and intense warming conditions. In this regard, it would be interesting also to determine the future evolution of the events under different climate change scenarios, that may affect not only their intensity, but also their duration (Pereira et al., 2017). While some previous works already addressed a future situation of more frequent and intense HWs and the inverse pattern for CWs (Abaurrea et al., 2018), the knowledge about their atmospheric configurations will improve the predictability of the events at a seasonal scale, as made before only with statistical analysis (Lavaysse et al., 2019).

5. Conclusions

Using a high-resolution gridded dataset of daily temperature in mainland Spain, HW and CW events were identified from the combination of threshold exceedances of maximum and minimum temperatures in the same day. The number of annual events, their duration, and their intensity at seasonal and annual scales, were calculated to describe de spatial and temporal characteristics of these type of extreme events. Results showed:

- A varied number of annual events, being HWs more frequent (>2.5 events/year), especially in southern half of the IP;
- An approximate 4-day average duration of CWs and HWs, with longer occurrences in southeastern Mediterranean coast;
- A remarkable higher seasonal intensity (just considering the cold or warm season) of CWs indicating their higher impact on natural processes (e.g., plant development, wildlife dynamics, etc.);
- Contrasted annual intensities (considering temperature variations across a complete year) with higher impacts of HWs on southern half of IP and lower in north and coastal areas, and the inverse pattern in CW situations;
- A more frequent HWs occurrence, especially from early 80s, when the number of events, their duration, and intensity, became higher for HWs and lower for CWs.

The synoptic classification of days within HWs and CWs covering more than 50% of the territory (widespread events) divided the origins of the events in 9 atmospheric situations (weather types) for each one. HWs showed a clear general pattern of hot air masses coming from the Saharan desert to the south. Different variations in their composition and spatial configuration characterized early and common HWs. CWs are originated from continental winter cold and dry air masses coming from central Europe, whose source direction and final extent determines their intensity, being a N-NE-E intrusion a guarantee for an extreme cold event.

The spatial and temporal characterisation of HWs and CWs in mainland Spain, as well as the definition of their origins, constitute a highly valuable tool for region al management that allows for identifying priority action areas depending on the potential impacts on the territory. This first work detecting patterns and revealing risk areas, is the first step to an integrate analysis of temperature-based risk for the whole region. The main contribution of this work is to provide the tools and the data for a sustainable territorial management in which prediction of risks related to HW and CW events can be improved, and their potential impacts minimized, increasing the resilience of territories.

Author statement

Roberto Serrano-Notivoli: Conceptualization, Data Curation, Formal analysis, Investigation, Methodology, Software, Validation, Visualization, Writing - Original Draft, Funding acquisition, Writing - Review & Editing. **Marc Lemús-Cánovas:** Investigation, Methodology, Software, Validation, Writing - Review & Editing. **Samuel Barrao:** Formal analysis, Resources, Writing - Original Draft. **Pablo Sarricolea:** Investigation, Formal analysis, Writing - Original Draft. **Oliver Meseguer-Ruiz:** Investigation, Formal analysis, Writing - Original Draft, . **Ernesto Tejedor:** Conceptualization, Methodology, Validation, Writing-Review & Editing, Supervision.

Declaration of competing interest

The authors declare that they have no known competing financial interests or personal relationships that could have appeared to influence the work reported in this paper.

Acknowledgments

RSN, SB and ET are supported by the Government of Aragón through the "Program of research groups" (group H09_20R, "Climate, Water, Global Change, and Natural Systems"). SB holds a pre-doctoral grant from the Government of Aragón. MLC, PS and OMR thank the Climatology Group (2017SGR1362, Catalan Government). The present research was also conducted within the framework EXE project (PID2020-116860RB-C21). M.L-C was awarded a pre-doctoral FPU Grant (FPU2017/02166) from the Spanish Ministry of Science, Innovation and Universities. ET was partially supported by NSF-Partnerships for International Research and Education (OISE-1743738), and by NSF-P2C2 (AGS-1702439). RSN was partially supported by the Universidad Autónoma de Madrid and the Comunidad de Madrid through project SI3-PJI-2021-00398.

Appendix A. Supplementary data

Supplementary data to this article can be found online at https://doi.org/10.1016/j.wace.2022.100471.

References

Abaurrea, J., Asín, J., Cebrián, A.C., 2018. Modelling the occurrence of heat waves in maximum and minimum temperatures over Spain and projections for the period 2031-60. Global and Planet. Change 161, 244–260. https://doi.org/10.1016/j.gloplacha.2017.11.015.

Acero, F.J., Fernández-Fernández, M.I., Carrasco, Sánchez V.M., Parey, S., Huon Huang, T.T., Dacunha-Castelle, D., García, J.A., 2017. Changes in heat wave characteristics over Extremadura (SW Spain). Theor. Appl. Climatol. 133, 605–617. https://doi.org/10.1007/s00704-017-2210-x.

AghaKouchak, A., Chiang, F., Huning, L.S., Love, C.A., Mallakpour, I., Mazdiyasni, O., Moftakhari, H., Papalexiou, S.M., Ragno, E., Sadegh, M., 2020. Climate extremes and compound hazards in a warming world. Annu. Rev. Earth Planet Sci. 48, 519–548. https://doi.org/10.1146/annurev-earth-071719-055228.

Allen, M.J., Sheridan, S.C., 2016. Spatio-temporal changes in heat waves and cold spells: an analysis of 55 U.S. cities. Phys. Geogr. https://doi.org/10.1080/02723646.2016.1184078.

Bitencourt, D.P., Fuentes, M.V., Franke, A.E., Silveira, R.B., Alves, M.P.A., 2020. The climatology of cold and heat waves in Brazil from 1961 to 2016. Int. J. Climatol. 40 (4), 2464–2478. https://doi.org/10.1002/joc.6345.

Burt, S., 2004. The August 2003 heatwave in the United Kingdom: Part 1 –Maximum temperatures and historical precedents. Weather 59 (8), 199–208. https://doi.org/10.1256/wea.10.04A.

Carmona, R., Díaz, J., Mirón, I.J., Ortíz, C., Linares, C., 2016. Geographical variation in relative risks associated with cold waves in Spain: the need for a cold wave prevention plan. Environ. Int. 88, 103–111. https://doi.org/10.1016/j.envint.2015.12.027.

Cattell, R.B., 1966. The Scree test for the number of factors. Multivariate Behav. Res. 1 (2), 245–276. https://doi.org/10.1207/s15327906mbr0102_10.

Fink, A.H., Brücher, T., Krüger, A., Leckebisch, G.C., Pinto, J.G., Ulbrich, U., 2004. The 2003 European summer heatwaves and drought –synoptic diagnosis and impacts. Weather 59 (8), 209–216. https://doi.org/10.1256/wea.73.04.

Fischer, E., Schär, C., 2010. Consistent geographical patterns of changes in high-impact European heatwaves. Nat. Geosci. 3, 398–403. https://doi.org/10.1038/ngeo866.

González-Hidalgo, J.C., Beguería, S., Peña-Angulo, D., Sandonis, L., 2021. Variability of maximum and minimum monthly mean air temperatures over mainland Spain and their relationship with low-variability atmospheric patterns for period 1916–2015. Int. J. Climatol. https://doi.org/10.1002/joc.7331.

Gutiérrez, J.M., San-Martín, D., Brands, S., Manzanas, R., Herrera, S., 2013. Reassessing statistical downscaling techniques for their robust application under climate change conditions. J. Clim. 26 (1), 171–188. https://doi.org/10.1175/JCLI-D-11-00687.1.

Hersbach, H., Bell, B., Berrisford, P., Hirahara, S., Horányi, A., Muñoz-Sabater, J., Nicolas, J., Peubey, C., Radu, R., Schepers, D., Simmons, A., Soci, C., Abdalla, S., Abellan, X., Balsamo, G., Bechtold, P., Biavati, G., Bidlot, J., Bonavita, M., De Chiara, G., Dahlgren, P., Dee, D., Diamantakis, M., Dragani, R., Flemming, J., Forbes, R., Fuentes, M., Geer, A., Haimberger, L., Healy, S., Hogan, R.J., Hólm, E., Janisková, M., Keeley, S., Laloyaux, P., Lopez, P., Lupu, C., Radnoti, G., de Rosnay, P., Rozum, I., Vamborg, F., Villaume, S., Thépaut, J.-N., 2020. The ERA5 global reanalysis Q. J. R. Meteor. Soc. 146, 1999–2049. https://doi.org/10.1002/qj.3803.

Hu, L., Luo, J.-J., Huang, G., Wheeler, M.C., 2019. Synoptic features responsible for heat waves in central africa, a region with strong multidecadal trends. J. Clim. 32 (22), 7951–7970. https://doi.org/10.1175/JCLI-D-18-0807.1.

Insua-Costa, D., Lemus-Cánovas, M., Miguez-Macho, G., Llasat, M.C., 2021. Climatology and ranking of hazardous precipitation events in the western Mediterranean area. Atmos. Res. 255, 10552 https://doi.org/10.1016/j.atmosres.2021.105521.

Lavaysse, C., Cammalleri, C., Dosio, A., van der Schrier, G., Toreti, A., Vogt, J., 2018. Towards a monitoring system of temperature extremes in Europe. Nat. Hazards Earth Syst. Sci. 18, 91–104. https://doi.org/10.5194/nhess-18-91-2018.

Lavaysse, C., Naumann, G., Alfieri, L., Salamon, P., Vogt, J., 2019. Predictability of the European heat and cold waves. Clim. Dynam. 52, 2481–2495. https://doi.org/10.1007/s00382-018-4273-5.

Lemus-Canovas, M., Lopez-Bustins, J.A., Martin-Vide, J., Royé, D., 2019. synoptReg: an R package for computing a synoptic climate classification and a spatial regionalization of environmental data. Environ. Model. Software 118, 114–119. https://doi.org/10.1016/j.envsoft.2019.04.006.

Lemus-Canovas, M., Lopez-Bustins, J.A., Martín-Vide, J., Halifa-Marin, A., Insua-Costa, D., Martinez-Artigas, J., Trapero, L., Serrano-Notivoli, R., Cuadrat, J.M., 2021. Characterisation of extreme precipitation events in the pyrenees: from the local to the synoptic scale. Atmosphere 12, 665. https://doi.org/10.3390/atmos12060665.

Lemus-Canovas, M., Lopez-Bustins, J.A., 2021. Assessing internal changes in the future structure of dry–hot compound events: the case of the Pyrenees. Nat. Hazards Earth Syst. Sci. 21, 1721–1738. https://doi.org/10.5194/nhess-21-1721-2021.

Liu, J., Ren, Y., Tao, H., Shalamzari, M.J., 2021. Spatial and temporal variation characteristics of heatwaves in recent decades over China. Rem. Sens. 13, 3824. https://doi.org/10.3390/rs13193824.

Lorenzo, N., Díaz-Poso, A., Royé, D., 2021. Heatwave intensity on the iberian Peninsula: future climate projections. Atmos. Res. 258, 105655 https://doi.org/10.1016/j.atmosres.2021.105655.

Merino, A., García-Ortega, E., Navarro, A., Fernández-González, S., Tapiador, F.J., Sánchez, J.L., 2021. Evaluation of gridded rain-gauge-based precipitation datasets: impact of station density, spatial resolution, altitude gradient and climate. Int. J. Climatol. 41 (5), 3027–3043. https://doi.org/10.1002/joc.7003.

Mohammed, A.J., Alarcón, M., Pino, D., 2018. Extreme temperature events on the Iberian Peninsula: statistical trajectory analysis and synoptic patterns. Int. J. Climatol. 38, 5305–5322. https://doi.org/10.1002/joc.5733.

Montero, J.C., Miron, J.I., Criado, J.J., Linares, C., Díaz, J., 2010. Comparison between two methods of defining heat waves: a retrospective study in Castile-La Mancha (Spain). Sci. Total Environ. 408 (7), 1544–1550. https://doi.org/10.1016/j.scitotenv.2010.01.013.

Olcina-Cantos, J., Serrano-Notivoli, R., Miró, J., Meseguer-Ruiz, O., 2019. Tropical nights on the Spanish Mediterranean coast, 1950−2014. Clim. Res. 78, 225–236. https://doi.org/10.3354/cr01569.

Pascal, M., Wagner, V., Le Tertre, A., Laaide, K., Honoré, C., Bénichou, F., Beaudeau, P., 2013. Definition of temperature thresholds: the example of the French heat wave warning system. Int. J. Biometeorol. 57, 21–29. https://doi.org/10.1007/s00484-012-0530-1.

Patz, J., Campbell-Lendrum, D., Holloway, T., Foley, J.A., 2005. Impact of regional climate change on human health. Nature 438, 310–317. https://doi.org/10.1038/nature04188.

Pereira, S.C., Marta-Almeida, M., Carvalho, A.C., Rocha, A., 2017. Heat wave and cold spell changes in Iberia for a future climate scenario. Int. J. Climatol. 37 (15), 5192–5205. https://doi.org/10.1002/joc.5158.

Perkins, S.E., Alexander, L.V., Nairn, J.R., 2012. Increasing frequency, intensity and duration of observed global heatwaves and warm spells. Geophys. Res. Lett. 39 (20), L20714 https://doi.org/10.1029/2012GL053361.

Philipp, A., Beck, C., Huth, R., Jacobeit, J., 2016. Development and comparison of circulation type classifications using the COST 733 dataset and software. Int. J. Climatol. 36 (7), 2673–2691. https://doi.org/10.1002/joc.3920.

Plavcová, E., Kysely, J., 2019. Temporal characteristics of heat waves and cold spells and their links to atmospheric circulation in EURO-CORDEX RCMs. Adv. Meteorol., 2178321 https://doi.org/10.1155/2019/2178321.

Prieto, L., García Herrera, R., Díaz, J., Hernández, E., del Teso, T., 2004. Minimum extreme temperatures over Peninsular Spain. Global Planet. Change 44, 59–71. https://doi.org/10.1016/j.gloplacha.2004.06.005.

Radinović, D., Ćurić, M., 2012. Criteria for heat and cold wave duration indexes. Theor. Appl. Climatol. 107, 505–510. https://10.1007/s00704-011-0495-8.

Richman, M., 1986. Review article, rotation of principal components. J. Climatol. 6, 293–335. https://doi.org/10.1002/joc.3370060305.

Robinson, P.J., 2001. On the definition of a heat wave. J. Appl. Meteorol. 40 (4), 762–775. https://doi.org/10.1175/1520-0450(2001)040%3C0762:OTDOAH%3E2.0.CO;2.

Sánchez-Benítez, A., Barriopedro, D., García-Herrera, R., 2020. Tracking Iberian heatwaves from a new perspective. Weather Clim. Extrem. 28, 100238 https://doi.org/10.1016/j.wace.2019.100238.

Serrano-Notivoli, R., Beguería, S., de Luis, M., 2019. STEAD: a high-resolution daily gridded temperature dataset for Spain. Earth Syst. Sci. Data 11, 1171–1188. https://doi.org/10.5194/essd-11-1171-2019.

Serrano-Notivoli, R., Tejedor, E., 2021. From rain to data: a review of the creation of monthly and daily station-based gridded precipitation datasets. WIRES Water 8 (6), e1555. https://doi.org/10.1002/wat2.1555.

Smith, T.T., Zaitchik, B.F., Gohlke, J.M., 2013. Heat waves in the United States: definitions, patterns and trends. Clim. Change 118 (3–4), 811–825. https://doi.org/10.1007/s10584-012-0659-2.

Sousa, P.M., Barriopedro, D., Ramos, A.M., García-Herrera, R., Espírito-Santo, F., Trigo, R.M., 2019. Saharan air intrusions as a relevant mechanism for Iberian heatwaves: the record breaking events of August 2018 and June 2019. Weather Clim. Extrem. 26, 100224 https://doi.org/10.1016/j.wace.2019.100224.

Spinioni, J., Lakatos, M., Szentimrey, T., Bihari, Z., Szalai, S., Vogt, J., Antofie, T., 2015. Heat and cold waves trends in the Carpathian Region from 1961 to 2010. Int. J. Climatol. 35 (14), 4197–4209. https://doi.org/10.1002/joc.4279.

Tan, J., Zheng, Y., Tang, X., Guo, C., Li, L., Song, G., Zhen, X., Yuan, D., Kalkstein, A.J., Li, F., Chen, H., 2010. The urban heat island and its impact on heat waves and human health in Shanghai. Int. J. Biometeorol. 54, 75–84. https://doi.org/10.1007/s00484-009-0256-x.

Viceto, C., Cardoso, S., Rocha, A., 2019. Climate change projections of extreme temperatures for the iberian Peninsula. Atmosphere 10, 229. https://doi.org/10.3390/atmos10050229.

Zschenderlein, P., Fink, A.H., Pfahl, S., Wernli, H., 2019. Processes determining heat waves across different European climates. Int. J. Climatol. 145 (724), 2973–2989. https://doi.org/10.1002/qj.3599.